Lab on a Chip

PAPER

Cite this: *Lab Chip*, 2020, **20**, 2520

Bacteria encapsulation and rapid antibiotic susceptibility test using a microfluidic microwell device integrating surface-enhanced Raman scattering†

Hsiu-Kang Huang,[a] Ho-Wen Cheng,[b] Cheng-Chieh Liao,[a] Shang-Jyun Lin,[a] Yi-Zih Chen,[c] Juen-Kai Wang,[bde] Yuh-Lin Wang [bf] and Nien-Tsu Huang *[ag]

The antibiotic susceptibility test (AST) is a general laboratory procedure for bacterial identification and characterization and can be utilized to determine effective antimicrobials for individual patients. Due to the low bacterial concentration, conventional AST usually requires a prolonged bacterial culture time and a labor-intensive sample pretreatment process. Therefore, it cannot perform timely diagnosis or treatment, which results in a high mortality rate for seriously infected patients. To address this problem, we developed a microfluidic microwell device integrating surface-enhanced Raman scattering (SERS) technology, or the so called the Microwell-SERS system, to enable a rapid and high-throughput AST. Our results show that the Microwell-SERS system can successfully encapsulate bacteria in a miniaturized microwell with a greatly increased effective bacteria concentration, resulting in a shorter bacterial culture time. By attaching a microchannel onto the microwell, a smooth liquid and air exchange can purify the surrounding buffer and isolate bacteria in an individual microwell for independent SERS measurement. For proof-of-concept, we demonstrated a 2 h AST on susceptible and resistant *E. coli* and *S. aureus* with a concentration of 10^3 CFU mL^{-1} in the Microwell-SERS system, whereas the previous SERS-AST method required 10^8 CFU mL^{-1} bacterial suspension droplets dispensing on a SERS substrate. Based on the above features, we envision that the Microwell-SERS system could achieve highly sensitive, label-free, bacteria detection and rapid AST to enable timely and accurate bacterial infection disease diagnosis.

Received 27th April 2020,
Accepted 5th June 2020

DOI: 10.1039/d0lc00425a

rsc.li/loc

Introduction

Accurate identification and characterization of microorganisms are essential for environmental monitoring, the food industry, and clinical diagnosis. For bacterial-induced infection diagnosis or disease treatment, the antibiotic susceptibility test (AST) is a general laboratory procedure to determine effective antimicrobials for individual patients. It can facilitate the proper selection of antibiotic treatment and prevent any overuse or misuse of antibiotics.[1,2] To perform AST on a clinical blood sample ($<10^{3-4}$ CFU mL^{-1} of pathogens), a 1–3 day blood culture time is usually required to increase the bacteria concentration for manual AST, such as the broth microdilution test, disk diffusion test or automated AST, operated using commercially available instruments (*e.g.* MicroScan WalkAway (Siemens Healthcare Diagnostics), Vitek 2 system (bioMe'rieux), Sensititre ARIS 2X (Trek Diagnostic Systems), and BD Phoenix automated microbiology system (BD Diagnostics)).[3–5] Although current manual or automated AST methods are cost-efficient, rapid and sensitive, they still require prolonged bacterial enrichment and labor-intensive sample preparation steps. Therefore, it cannot provide a timely treatment and diagnosis, thereby resulting in a high mortality rate for seriously infected patients with severe bacterial infectious diseases like sepsis.[6,7]

Besides the above AST methods, various miniaturized sensors have been developed for direct bacteria counting or observation of antibiotic-treated bacteria growth to determine

[a] *Graduate Institute of Biomedical Electronics and Bioinformatics, National Taiwan University, Taipei, Taiwan. E-mail: nthuang@ntu.edu.tw*
[b] *Institute of Atomic and Molecular Sciences, Academia Sinica, Taipei, Taiwan*
[c] *Department of Biomechatronics Engineering, National Taiwan University, Taipei, Taiwan*
[d] *Center for Condensed Matter Sciences, National Taiwan University, Taipei, Taiwan*
[e] *Center for Atomic Initiative for New Materials, National Taiwan University, Taipei, Taiwan*
[f] *Department of Physics, National Taiwan University, Taipei, Taiwan*
[g] *Department of Electrical Engineering, National Taiwan University, Taipei, Taiwan*
† Electronic supplementary information (ESI) available. See DOI: 10.1039/d0lc00425a

the minimal inhibitory concentration (MIC). The sensing mechanisms include (1) mechanical (microcantilever[8,9]); (2) optical (cell phone-based microphotometric systems,[10] colorimetric assay,[11] fluorescence,[12] microdroplets,[13] surface-enhanced Raman spectroscopy (SERS) sensing[14–17]); (3) magnetic (magnetic bead rotation[18]); (4) electrical (microfluidic electrical impedance spectroscopy (m-EIS),[19] electrical resistance[20]) or (5) thermal (isothermal microcalorimetry (IMC)[21]) systems. By further integrating with microfluidics, these systems can better isolate or confine bacteria in a microenvironment for precise and sensitive bacterial counting or identification. For example, previous research utilized a microfluidic agarose channel to confine bacterial suspensions under various drug concentration treatments and microscopically analyze the bacterial count to determine the susceptibility.[22,23] The second example is based on inertial microfluidics to isolate bacteria from whole blood and directly determine their identity and antibiotic susceptibility with hybridization-based RNA detection.[24] Although the nucleic acid based method allows the direct identification of low abundance pathogens (~100 CFU mL^{-1}) without any post-culture or enzymatic amplification, false positive and false negative results may happen without proper sequence design. The third example integrates a microchamber with an atomic force microscope (AFM) cantilever[8] or a microchannel with a microcantilever[9] functionalized with receptors to selectively capture bacteria passing through the channel and measure the corresponding deflection or resonance frequency shift. Compared to the above techniques, the SERS technique has been proposed for microbial characterization based on its label-free, highly-specific, and accurate sensing features. A comprehensive review of SERS-based bacteria identification, functional analysis of microorganisms, complex biofilm characterization and AST has been shown in previous studies.[14,15] By comparing the characteristic Raman signal change of bacteria-secreted metabolites before and after antibiotic treatment, the SERS-AST method could accurately determine the MIC in 2 h and would not be affected by the issue of bacteria aggregation and uneven distribution.[16,17]

Although the SERS-AST method can easily obtain highly-sensitive bacterial Raman spectra, due to the extremely sensitive features of SERS technology, an extra sample purification process is usually required to prevent any background signal interference.[6,25] Besides, the low bacterial count is an issue to perform a meaningful SERS spectrum measurement. To address the above issues, various microencapsulation methods have been demonstrated to enrich bacteria in the enclosed sensing region, leading to an increased effective bacteria concentration. Current microencapsulation methods can be categorized into four types: (1) microvalve; (2) microdroplet; (3) membrane, and (4) microwell. The first method uses pneumatic microvalves to create a microchamber for single *E. coli* encapsulation.[26] After bacteria isolation, the system can then perform single-cell genome amplification on a nanoliter scale. The second method uses microfluidics to generate microdroplets to encapsulate bacteria in nanoliter-sized plugs.[27] Since bacteria are stochastically encapsulated in microdroplets, an additional sorting process is required. The third method utilizes a microfluidic device embedded membrane filter for bacteria enrichment followed by *in situ* SERS measurement.[17] The last method performs stochastic bacteria encapsulation in a microwell array.[28] High-throughput bacterial growth with controlled physical and chemical parameters can be observed in the system. The authors found that seeding bacteria in microwells with different sizes may lead to a homogenous (large size) or heterogeneous (small size) population assembly.

In this paper, we report a microfluidic microwell device integrating a SERS substrate (Microwell-SERS system) for bacteria isolation, followed by enrichment and *in situ* AST (Fig. 1). Here, a microwell is utilized for bacteria encapsulation based on two reasons. First, compared to a microvalve or membrane design, a microwell can directly become an individual microenvironment without any microvalve control. Furthermore, the highly-dense microwell (100 wells per mm^2) layout can potentially perform multiple parallel ASTs with different antibiotic concentrations or bacteria strains. The second reason is the ease-of-integration of the SERS substrate with the microwell. Since the microwell device can be made of a thin and highly-transparent layer, it has minimal Raman signal interference when it is directly attached to the SERS substrate. To achieve rapid and efficient bacteria encapsulation, the microwell device is placed in an ultracentrifuge tube. Similar to the standard centrifugation procedure, bacteria are dispersed into the microwells based on the centrifugal force. After trapping bacteria in the microwells, a microchannel is placed on top of the microwells to isolate each microwell for on-chip bacteria cultivation. Finally, the SERS substrate, replacing the microchannel, is attached to the microwells for *in situ* SERS measurement. In summary, the Microwell-SERS system can greatly increase the effective bacteria concentration, resulting in a shorter bacterial culture time and a stronger SERS signal in AST. The well-confined liquid-phase microenvironment in the microwells also enables uniform SERS measurement of bacteria-secreted metabolites after antibiotic treatments. Based on the above features, we envision that this Microwell-SERS system can be a rapid, uniform, sensitive, and high-throughput bacteria AST detection platform, which would benefit various bacteria related infectious disease diagnosis.

Materials and methods

Bacteria and antibiotics

Both *E. coli* (ATCC 25922) and *S. aureus* (ATCC 25923) were purchased from the American Type Culture Collection (ATCC) and were used as susceptible strains. *E. coli* (DH5-Alpha) transfected with a kanamycin-resistant plasmid and *S. aureus* (HG001) transfected with a chloramphenicol-resistant plasmid served as resistant strains. For validating the

bacteria trapping efficiency, both *E. coli* and *S. aureus* were transfected with the green fluorescent protein (GFP) for fluorescence imaging. The antibiotics kanamycin and chloramphenicol were both purchased from Sigma-Aldrich. All bacteria samples were cultured in Mueller–Hinton broth (MHB, BD BBL).

Bacterial growth and preparation

To adjust the bacteria concentration, bacteria were first re-solubilized in 5 mL of MHB and incubated in an orbital shaking incubator operated at 200 rpm and 37 °C for 16–18 h. Then, a 0.2 mL overnight-cultured sample was added into another 5 mL of MHB for 2 h incubation to reach the exponential phase. The bacteria sample was next diluted into 10^8 CFU mL^{-1} based on its optical density and bacteria plating results. To validate the lowest bacteria trapping concentration, the bacteria sample was serially diluted to lower concentrations (10^2 to 10^7 CFU mL^{-1}) with MHB. All bacteria samples were prepared inside a laminar flow cabinet at room temperature and proper biosafety regulations were followed.

The Microwell-SERS device fabrication

The microwell and microchannel devices were both fabricated using the soft lithography process similar to our previous study.[29] Briefly, a silicon mold was first fabricated using the photolithography process. Then, PDMS (Sylgard-184, Dow Corning) prepolymer, with a 1 : 10 weight ratio of the PDMS curing agent to the base monomer, was mixed with 3% silicone oil to facilitate the subsequent release of patterned PDMS layers. After being stored in a 60 °C oven for 2 h, fully cured PDMS structures were peeled off from the silicon mold. The SERS substrate was fabricated by following by our previous protocol.[17] Briefly, a glass slide was first pre-cleaned with acetone and sodium hydroxide and then silver-island-film coated with an average thickness of 7 nm using an E-beam evaporator (EBS-300, Junsun Tech) at a 0.3 nm min^{-1} evaporation rate. The microchannel and SERS substrate were temporarily attached onto the top of the microwell device based on the electrostatic force during the bacterial isolation and SERS measurement, respectively.

The operational protocol of the Microwell-SERS system

The operational protocol of the Microwell-SERS system is shown in Fig. 2. Generally, it can be divided into seven steps. First, the bacteria sample was incubated with an antibiotic for 2 h (step 1). Then, the sample was centrifuged at 10 000 relative centrifugal force (RCF) for 2 min at room temperature to form a bacterial pellet. Then, the MHB culture medium suspension was replaced by deionized (DI) water (step 2). The DI washing process would force the bacteria into the starvation stage and secreting more metabolites of purine degradation, such as adenine, hypoxanthine, xanthine, guanine, uric acid, and adenosine monophosphate. This DI washing process has been reported previously[30,31] and no bacteria rupture results were observed. This step was repeated three times to completely wash out the remaining culture medium, preventing any SERS signal interference. Next, a 9 mL bacteria sample in DI water was loaded into the ultracentrifuge tube equipped with the microwell device fixed with a poly(methyl methacrylate) (PMMA) holder and rotated at 8000 RCF for 5 min to disperse the bacteria into the microwells (step 3). Then, the microwell device was retrieved from the tube and air-dried for 5 min (step 4). Next, DI water was loaded into the device to rehydrate the microwells and create a nutrient-deficient microenvironment (step 5). Then, 200 μL of air was loaded into the device to remove the residual DI water in the microchannel and create an individual microwell for bacterial culture (step 6). Finally, the microchannel was replaced by the SERS substrate for *in situ* SERS measurement (step 7).

Bacteria encapsulation in the microwells

GFP-transfected *E. coli* and *S. aureus* encapsulated in the microwells were counted under a fluorescence microscope (IX-73, Olympus) with a 10× objective lens. A sequence of

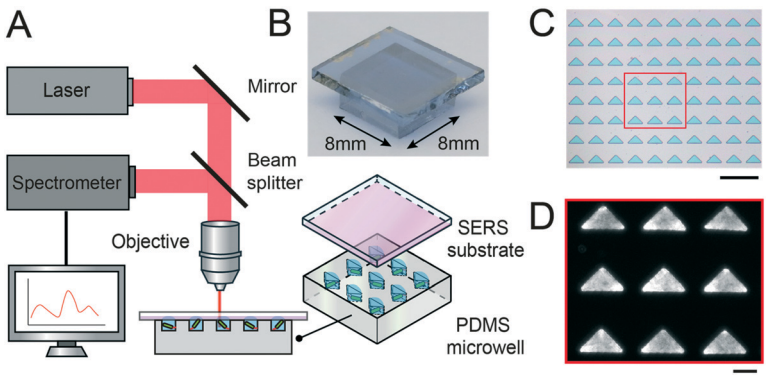

Fig. 1 The Microwell-SERS system: (A) schematic diagram of the system, including Raman microscopy and the Microwell-SERS device; (B) photo of the microwell device attached with a SERS substrate with the SERS-active surface (in purple) facing downward; (C) bright-field image of the microwells rehydrated with blue food dye (scale bar, 200 μm); (D) fluorescence image of 10^6 CFU mL^{-1} GFP-transfection bacteria confined in nine microwells (scale bar, 50 μm).

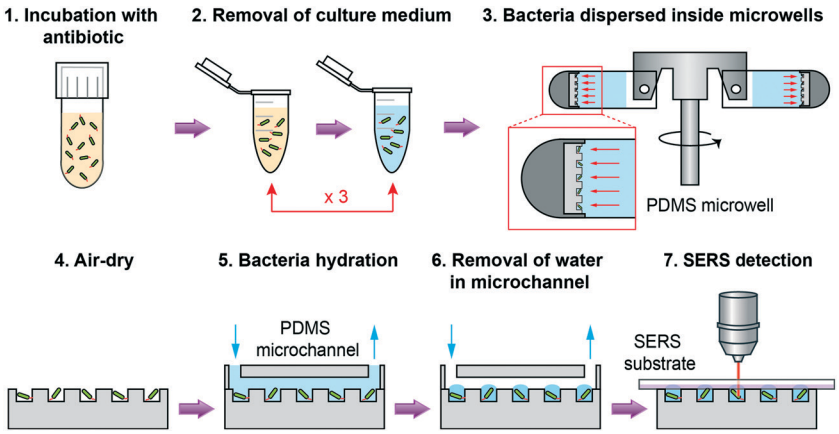

Fig. 2 Operation protocol of the microwell-SERS device: (1) incubation with antibiotic – bacteria (green ovals) are incubated with an antibiotic for 2 h in the bacterial culture tube; (2) removal of culture medium – the culture medium (yellow) is washed away (three times) with DI water (blue); (3) bacteria dispersed inside microwells – the bacteria solution is then loaded into an ultracentrifuge tube equipped with the microwell device to concentrate bacteria into the microwells; (4) air-dry – the microwell device is air-dried for PDMS microwell attachment; (5) bacteria hydration – the microwell device is then rehydrated with DI water. The bacteria not seeded inside the microwells will also be washed away; (6) removal of water in microchannel – air is flowed through the microchannel to isolate each microwell for metabolite secretion; (7) SERS detection – the SERS substrate was attached onto the microwell device for SERS measurement.

images, recorded using a dual-color charge-coupled device (CCD) (DP-80, Olympus) with an integration time of 0.5 s, were obtained by raster-scanning the sample using a motorized stage MFD-2, Märzhäuser. The acquired images were then stitched with microscopy analysis software (CellSens, Olympus), yielding an 8 × 8 mm^2 combined image covering the whole microwell device. Since the trapped bacteria all aggregated to the corners of the triangle, we used the ImageJ software to calculate the average fluorescence intensity of 40 microwells to quantify the bacteria seeding performance.

SERS measurement and spectral processing

The Raman microscope (SuperHead HE 640, Horiba Jobin Yvon) is constructed with a standard epi-fluorescence microscope (BX61WI, Olympus) equipped with a 632.8 nm HeNe laser (LGK 7665 P18, LASOS) as the excitation source. The laser light was first filtered using a band-pass filter and then focused on the SERS substrate with a 50× objective lens. The scattered light was obtained with a 1 s integration time and collected by the same objective lens. Then, the light passed through a Raman long-pass filter and was sent to an 80 cm spectrograph (1200 gr mm^{-1}) with a liquid nitrogen-cooled CCD for spectral measurement. The resultant spectral resolution and error were 4 and 0.1 cm^{-1}, respectively. The laser irradiation power was 5 mW with an OD1 neutral density filter. For multiple microwell measurements, the device was raster-scanned using a motorized stage (EK 32, Märzhäuser). For each microwell, the SERS spectrum was averaged over 9 spots and processed using a baseline removal program based on the nonlinear iterative peak clipping algorithm.[32] Similar to our previous study,[31] the parameter r_{740}, as the signal ratio of I_{740} of bacteria treated with antibiotics divided by I_{740} of bacteria not treated with antibiotics $\left(r_{740} = \frac{I_{740,\text{treated}}}{I_{740,\text{not treated}}}\right)$, was used to determine the antibiotic susceptibility of the bacteria strains. The standard deviation of r_{740} is defined as $\delta(r_{740}) = r_{740} \times \sqrt{\left(\frac{\delta(I_{740,\text{treated}})}{I_{740,\text{treated}}}\right)^2 + \left(\frac{\delta(I_{740,\text{not treated}})}{I_{740,\text{not treated}}}\right)^2}$.

Results and discussion

The Microwell-SERS system design

As shown in Fig. 1, the Microwell-SERS system consists of (1) a polydimethylsiloxane (PDMS) triangular microwell device; (2) a SERS substrate, and (3) a Raman microscope. The overall microwell dimensions are 8 × 8 mm^2 with 6400 wells (Fig. 1B). The dimensions of a single triangular microwell are 80 μm width (W), 40 μm length (L) and 20 μm depth (D) with an equivalent volume of 32 pL. Such an extremely small volume can greatly increase the effective bacteria concentration. For example, if one bacterium is trapped in the 32 pL microwell, the equivalent bacteria concentration would be 3 × 10^7 bacteria per 1 mL. To reach this concentration level in a milliliter scale container, a prolonged bacteria culture time (16 h) is usually required. The triangular microwell shape allows better bacterial observation in the low concentration case since bacteria would aggregate to the corners during the ultracentrifugation and air-drying processes. Fig. S1† compares the fluorescence of 10^4 CFU mL^{-1} GFP-transfected bacteria encapsulated in the triangular and circular microwells with the same microwell dimensions and density. Fig. 1C shows that the blue dye solution was uniformly distributed in the microwells after the rehydration and air-drying processes (steps 5 & 6 in Fig. 2). Fig. 1D shows the fluorescence image of 10^6 CFU mL^{-1} GFP-transfected *E. coli* evenly encapsulated in the microwells following the

operation protocol (steps 3–6 in Fig. 2). The clear fluorescence profile indicates that bacteria outside the microwells can be completely washed out in step 6, Fig. 2.

Bacteria trapping efficiency

To determine the bacteria trapping efficiency using the microwell device, we loaded 9 mL of GFP-transfected *E. coli* at 10^2 to 10^6 CFU mL^{-1} into the ultracentrifuge tube equipped with the microwell device (steps 3 and 4 in Fig. 2). After 8000*g* centrifugation for 5 min, we took fluorescence images of the bacteria seeded inside the microwell device. Next, we air-dried the microwell device to allow bacteria to attach onto the edges and the bottom surface of the microwells for better imaging. For each bacteria concentration case, we took the fluorescence images of 40 microwells and the average intensity using ImageJ software. Fig. 3A shows the microwell images at each concentration (10^2–10^6 CFU mL^{-1}), where the yellow dashed lines represent the microwell boundary. At low bacteria concentrations (10^2–10^4 CFU mL^{-1}), most bacteria were seeded on the edges of the microwell and cannot easily be observed. As the bacteria concentration increased to 10^5 CFU mL^{-1}, a clear bacteria seeding pattern was observed. Once the bacteria concentration reached 10^6 CFU mL^{-1}, the microwell is fully occupied, indicating the capacity limit of the microwell. Fig. 3B shows the corresponding fluorescence intensity (I_{fl}) at different bacteria concentrations ($C_{E.c}$). At 10^2 CFU mL^{-1}, the fluorescence intensity cannot be statistically differentiated from the background (the intensity outside the microwell), whereas at 10^3 CFU mL^{-1}, it can statistically be differentiated from the 10^2 CFU mL^{-1} case, representing the detectable concentration limit by fluorescence imaging. Based on these results, we decided to use 10^3 CFU mL^{-1} as the initial bacteria concentration for following SERS-AST.

Adenine measurement using the Microwell-SERS system

One important feature of the Microwell-SERS system is the rapid molecular diffusion into the SERS substrate due to its shorter well height. However, the miniaturized sample volume in the microwells may lead to less molecular binding to the SERS substrate. To compare the SERS signal variance in micro- and macro-environments, we selected various concentrations (10^{-4} to 10^{-9} M) of adenine as the target molecule and then dispensed them into 32 pL microwells or formed 2 μL microdroplets on the SERS substrate. The corresponding SERS signals from the microwells and microdroplets are shown in Fig. 4A and B, respectively. The black line represents the SERS spectrum of DI water as the background signal. To quantify the correlation of SERS signals *versus* the adenine concentration, we selected the characteristic Raman peak of adenine (740 cm^{-1}), extracted its intensity as I_{740} (yellow highlight bar) and plotted it as a function of the adenine concentration, as shown in Fig. 4C. Besides the 740 cm^{-1} peak, we also found that there are some other peaks between 920–950 cm^{-1} and 1200–1400 cm^{-1} as shown in the microwell case. We suspect that these signals may come from the molecules secreted from the PDMS microwells since we did not observe these peak signals in the microdroplet case (no PDMS microwells). However, these signals would not affect the intensity of the 740 cm^{-1} peak, the major Raman signal of adenine. Overall, the sensitivity of the microdroplets in the dynamic range of 10^{-5} to 10^{-8} M is slightly higher than that in the microwell case in the dynamic range of 10^{-4} to 10^{-7} M. This may be due to less molecule binding to the SERS substrate in the microwell case (the volume is 6.25 × 10^4 times lower while the surface area is just 3000 times lower).

SERS measurement for bacteria encapsulation in microwells

The second important feature of the Microwell-SERS system is the highly-dense and independent microwell array, which allows multiple parallel SERS measurements. To enable this feature, a uniform and large-area SERS substrate is also required. Compared to nanoparticle-based SERS probes, the nanostructure-based SERS substrate is believed to have a higher sensing uniformity and reproducibility since it has a more uniform nanostructure arrangement and would not

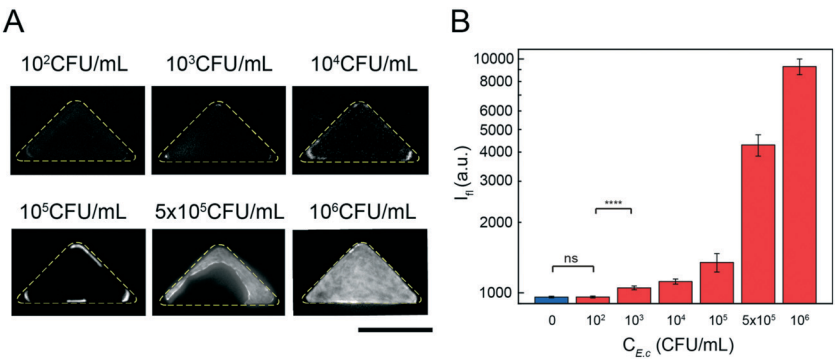

Fig. 3 (A) Representative fluorescence images of a microwell encapsulating different bacterial concentrations and (B) the quantified fluorescence intensity of the microwell-encapsulated bacteria at different concentrations (10^2 to 10^6 CFU mL^{-1}) (****: *p*-value < 0.0001; ns: statistically not significant) (scale bar, 50 μm).

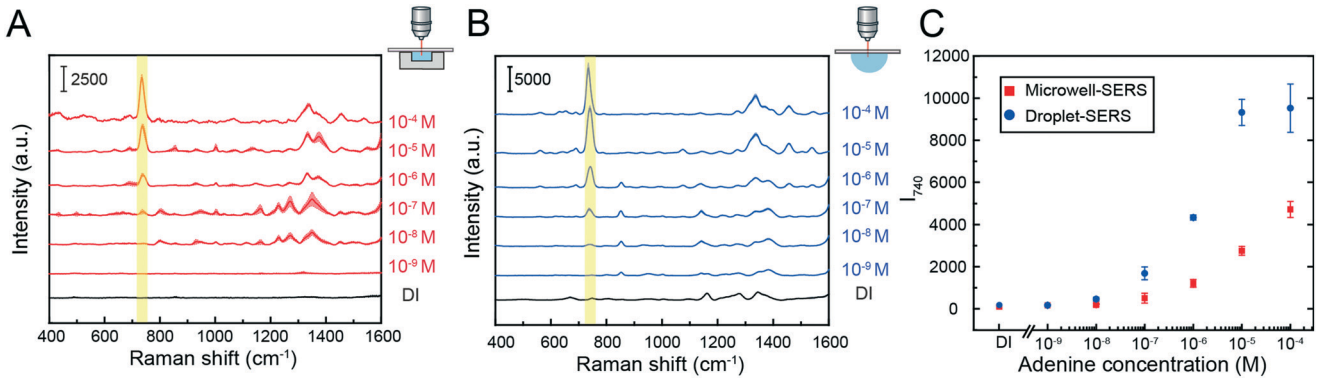

Fig. 4 (A–C) SERS spectra of adenine in water at concentrations ranging from 10^{-4} to 10^{-9} M using (A) 32 pL microwells and (B) 2 μL microdroplets on the SERS substrate; (C) the comparison of the Raman signal at 740 cm^{-1} (highlighted with yellow in the SERS spectra) plotted as a function of the adenine concentration in (A) and (B). The standard deviations were obtained from multiple samples.

suffer from nanoparticle aggregation issues. To ensure that the bacteria can be uniformly trapped in the microwell array and detected by multiple parallel SERS measurements, we performed a Raman mapping test using 10^5 CFU mL^{-1} bacteria encapsulated in the microwells and measured the corresponding SERS signals. Since the signal strength of I_{740} (yellow highlight bar) is the most prominent Raman spectrum feature of the bacteria-secreted metabolites, adenine and hypoxanthine, we chose this peak intensity to quantify the bacteria inside the microwells.[17] To ensure the highest sensing resolution, we collected the complete Raman signal inside and outside the microwells (20 sensing spots in one microwell) at 10 μm pixel resolution. The whole scanning area is 0.33 mm × 0.33 mm, covering 9 microwells. Then, we calculated the 740 cm^{-1} Raman peak intensity and plotted the Raman mapping image in grayscale. As shown in Fig. 5, it is clear that the bacteria solution in the top-right microwell leaked out during the SERS substrate attachment process, indicating a weaker Raman signal inside the microwell. Such a case could easily be excluded based on the significantly lower signal. Besides this microwell, the other 8 microwells showed a uniform and strong Raman intensity ($I_{740,\ \text{microwell}}$ = 785) compared to the Raman intensity outside the microwells ($I_{740,\ \text{background}}$ = 282). The signal-to-noise ratio ($I_{740,\ \text{microwell}}$/$I_{740,\ \text{background}}$) is around 2.78. Based on this Raman mapping result, we can confirm the feasibility of multiple parallel SERS measurements and the reproducibility of bacteria encapsulation in the microwell experiment.

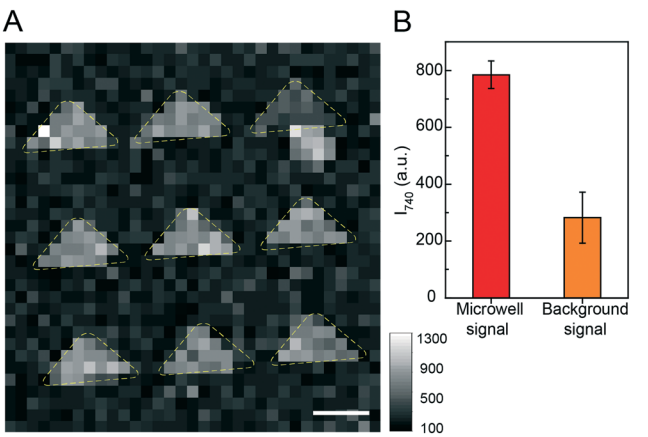

Fig. 5 (A) The 740 cm^{-1} Raman intensity mapping image of 10^5 CFU mL^{-1} *E. coli* encapsulated in 9 microwells. (B) The averaged Raman intensity inside and outside the microwells.

Antibiotic susceptibility test using the Microwell-SERS system

In our previous SERS-AST protocol,[31] bacteria required at least 2 h antibiotic treatment to identify susceptible or resistant strains. To confirm that the same protocol can be applied for the Microwell-SERS system, 10^8 CFU mL^{-1} *E. coli* was first cultured in MHB for 2 h and diluted to 10^3 CFU mL^{-1} based on the operation protocol (steps 1 and 2 in Fig. 2). Then, the sample was either subjected to the bacteria encapsulation procedure (steps 3–7 in Fig. 2) to perform SERS measurement in a microwell or dispensed as 2 μL microdroplets for SERS measurement. Besides the two different sample volumes, we also prepared two control samples: (1) pure DI water and (2) 10^3 CFU mL^{-1} *E. coli* without any culture time (directly replaced MHB by DI water) as a comparison. The corresponding SERS signals from the microwell and microdroplets are shown in Fig. 6. We found out that I_{740} after 2 h culture in the microwell showed a higher value compared to those of the other control samples. When comparing the 2 h cultured bacteria samples, the signal from the microwell is also stronger than the one in the microdroplet format. We believe that this is due to the bacteria confinement and enrichment in the microwell by using the centrifugation process and microwell confinement, since the surface-to-volume ratio is higher in the microwell case (1600 μm^2/32 pL = 5 × 10^4 m^{-1}) compared to that of a microdroplet (3.68 × 10^6 μm^2/2 μL = 1840 m^{-1}), which means the bacteria-secreted molecules would have a higher chance to interact with the SERS substrate. Based on the results of the bacteria seeding profiles and the corresponding Raman spectra, we selected 10^3 CFU mL^{-1} bacteria concentration as

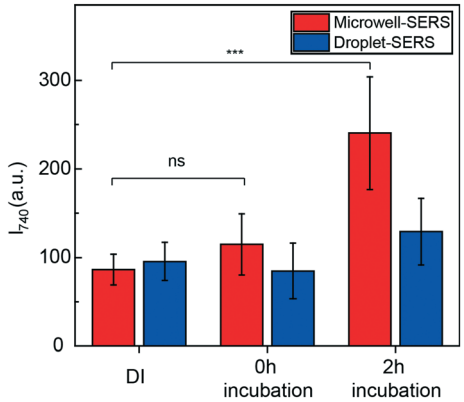

Fig. 6 The 740 cm^{-1} Raman intensities of pure DI water and 10^3 CFU mL^{-1} *E. coli* after 0 and 2 h incubation and processing by the bacteria encapsulation protocol in the microwells and microdroplets (***: *p*-value < 0.005, ns: not significant).

the minimum concentration for SERS-AST in our Microwell-SERS system.

Finally, we selected four bacteria strains: (1) resistant *E. coli*; (2) susceptible *E. coli*; (3) resistant *S. aureus*, and (4) susceptible *S. aureus*, as target samples. First, *E. coli* and *S. aureus* (OD = 0.5, equivalent to 10^8 CFU mL^{-1}) were treated (co-cultured) with or without kanamycin (16 μg mL^{-1}) and chloramphenicol (8 μg mL^{-1}) in a bacteria culture tube for 2 h. The selected antibiotic concentration was the standard concentration used to distinguish resistant strains according to the Clinical & Laboratory Standards Institute (CLSI) report. Next, 9 mL of *E. coli* and *S. aureus* solution diluted to 10^3 CFU mL^{-1} with DI water was loaded into the ultracentrifuge tube equipped with the microwell device for bacteria encapsulation. Then, the trapped bacteria were cultured with DI water inside the microwells for *in situ* SERS measurement. The SERS spectra for each condition were measured and averaged from 8–12 microwells. As shown in Fig. 7A, for the *E. coli* strains, I_{740} of the susceptible strain treated with 16 μg mL^{-1} kanamycin is considerably smaller than that without the treatment (red curves), while I_{740} of the resistant strain did not show a distinct difference before and after the

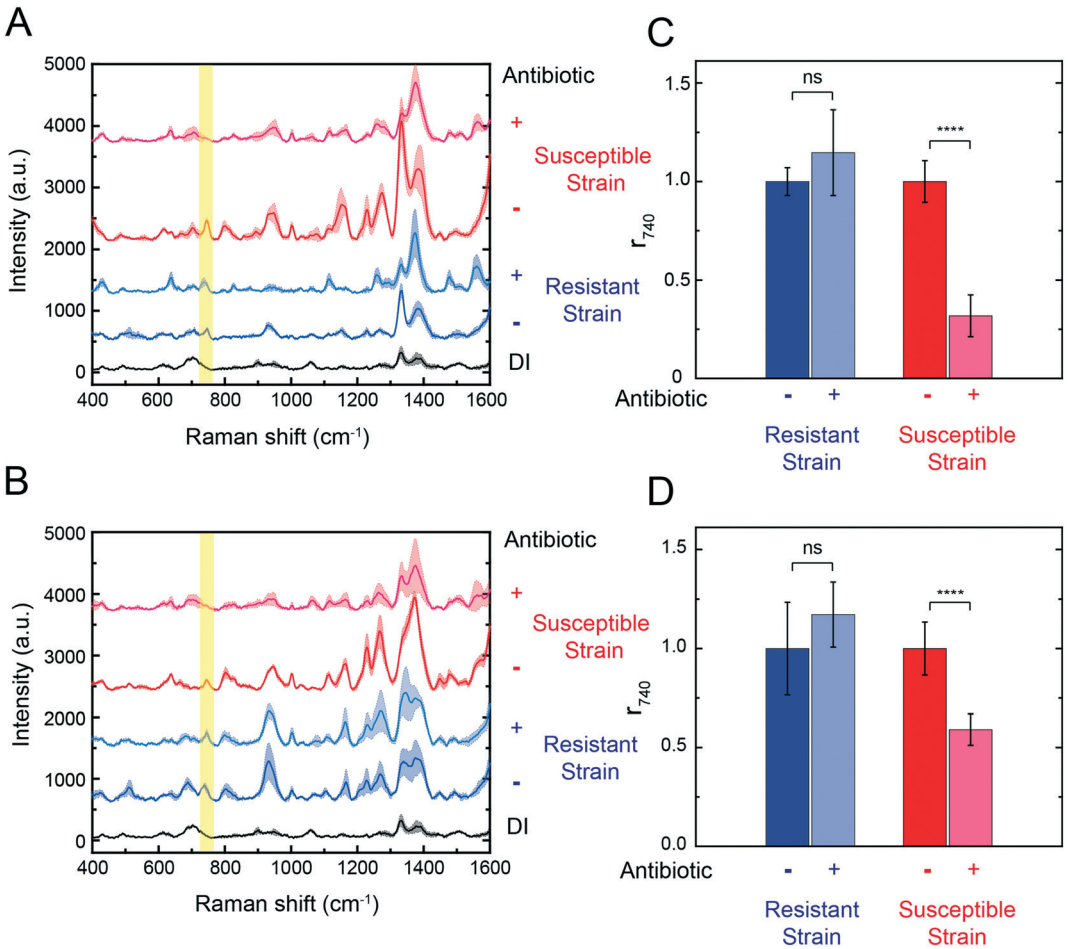

Fig. 7 Antibiotic susceptibility test results of *E. coli* and *S. aureus* treated with and without antibiotics in the Microwell-SERS system: (A) SERS spectra of susceptible and resistant *E. coli* treated with and without kanamycin at 16 μg mL^{-1}; (B) SERS spectra of susceptible and resistant *S. aureus* treated with and without chloramphenicol at 8 μg mL^{-1}; the black line in (A) and (B) is the average Raman spectrum of DI water for comparison. The light bands represent their corresponding standard deviations. (C and D) The ratios of the signal strengths at 740 cm^{-1} (r_{740}) of susceptible and resistant (C) *E. coli* and (D) *S. aureus* (***: *p*-value < 0.005, ns: not significant).

antibiotic treatment (blue curves). For the *S. aureus* strains (Fig. 7B), I_{740} of the susceptible strain treated with 8 μg mL^{-1} chloramphenicol showed a clear drop, while I_{740} of the resistant strain did not. To further quantify the signal difference between the susceptible and resistant *E. coli* and *S. aureus* strains, the r_{740} values of the susceptible *E. coli* and *S. aureus* strains after the antibiotic treatment were calculated to be 0.28 and 0.59, which are significantly smaller than those of the resistant strains (1.12 and 1.17) (Fig. 7C and D). The SERS-AST result showed that resistant or susceptible strains can be successfully identified using an initial bacterial concentration of 10^3 CFU mL^{-1}. To confirm our assay feasibility, we also did a bacteria culture experiment using the broth dilution method as the control experiment. Here, we selected the same four bacteria strains used in our SERS-AST test. The initial bacterial concentration is 5×10^5 CFU mL^{-1} as per the CLSI recommendation. Each *E. coli* and *S. aureus* strain was mixed with the corresponding antibiotics, kanamycin and chloramphenicol, respectively, at various concentrations (0–256 μg mL^{-1}). The total bacteria culture time is 15 h. As shown in Fig. S2,† we calculated the OD value of each bacteria strain at each antibiotic concentration and determined 1 and 256 μg mL^{-1} (red circle) as the MIC of susceptible and resistant *E. coli*, respectively, whereas 4 and 64 μg mL^{-1} is the MIC for susceptible and resistant *S. aureus*, respectively. Based on this control experiment result, 16 and 8 μg mL^{-1} was chosen as the critical concentration to distinguish if *E. coli* and *S. aureus* is susceptible or resistant. Overall, the control experiment showed the same trend compared to our SERS-AST test, confirming the assay feasibility.

Conclusions

In this paper, we developed the Microwell-SERS system for efficient bacteria encapsulation in microwells followed by *in situ* AST. The simplified two-layer microwell–SERS substrate structure can be easily placed on a Raman microscope for either fluorescence or Raman signal scanning. Our bacteria seeding fluorescence images showed the successful bacteria encapsulation and enrichment in microwells using the centrifugation and air-drying protocol. Then, we successfully measured the corresponding SERS spectra of bacteria-secreted metabolites in the microwells at an initial bacterial concentration of 10^3 CFU mL^{-1}. Compared to the conventional SERS-AST method using the centrifugation–purification protocol, the required initial bacteria culture time is much shorter. The SERS-AST assay reproducibility was confirmed by a high-resolution Raman mapping test. Finally, we demonstrated a 2 h AST on susceptible and resistant *E. coli* and *S. aureus* at 10^3 CFU mL^{-1}. The AST result is consistent with the standard bacterial culture experiment using the broth dilution method. Overall, there are three main features of our setup. First, the effective bacteria concentration can be greatly increased in the microwells, leading to a shorter bacterial culture time. Second, when bacteria are cultivated in the miniaturized microwell environment, the secreted molecules can efficiently diffuse to the SERS substrate for stronger and more uniform SERS signals. Lastly, the highly-dense (100 wells per mm^2) microwell array with a precise position arrangement can potentially be applied to multiple parallel ASTs for different bacteria types or multiple antibiotic concentration treatments. To achieve this function, a multi-branched microchannel or a microfluidic concentration gradient generator is required to be attached to the microwells.[12,33] Another improvement direction is to reduce the required initial bacteria concentration. Currently, if the initial bacteria concentration is too low ($<10^2$ CFU mL^{-1}), the bacteria encapsulation inside the microwells will be unevenly distributed. A potential solution is to use an image processing algorithm to pre-select microwells encapsulating more bacteria for following SERS measurement. If the above features can be successfully developed, we envision that this platform can be a rapid and sensitive tool for infectious bacteria disease diagnosis.

Author contributions

H.-K. Huang designed and performed the experiments, fabricated the microfluidic devices, analyzed the data, and prepared the manuscript; H.-W. Cheng provided SERS substrates and assisted in Raman measurement experiments; C.-C. Liao, S.-J. Lin and Y.-Z. Chen conducted bacteria culture, sample preparation, and data analysis and revised the manuscript; J.-K. Wang and Y.-L. Wang provided bacteria culture facilities, assisted in data analysis and wrote the manuscript; N.-T. Huang proposed the original idea, guided the experiments and wrote the manuscript.

Conflicts of interest

The authors declare no conflict of interest. The founding sponsors had no role in the design of the study; in the collection, analyses or interpretation of data; in the writing of the manuscript, and in the decision to publish the results.

Acknowledgements

This work was supported by the Ministry of Science and Technology, Taiwan under the grants "MOST 106-2221-E-002-058-MY3" and "MOST 106-2745-M-001-004-ASP". We are thankful to Dr. Li-Kwan Chang's lab for providing GFP-transfected *E. coli*, Dr. Mei-Hui Lin's lab for providing GFP-transfected *S. aureus*, Mr. Kuo-Kai Hsu for providing kanamycin-resistance transfected *E. coli*, and Dr. Chi-Hung Lin's lab for providing kanamycin.

References

1 I. Abubakar, L. Irvine, C. F. Aldus, G. M. Wyatt, R. Fordham, S. Schelenz, L. Shepstone, A. Howe, M. Peck and P. R. Hunter, *Health Technol. Assess.*, 2007, **11**, 1–216.

2 A. Ahmed, J. V. Rushworth, N. A. Hirst and P. A. Millner, *Clin. Microbiol. Rev.*, 2014, **27**, 631–646.
3 L. B. Reller, M. Weinstein, J. H. Jorgensen and M. J. Ferraro, *Clin. Infect. Dis.*, 2009, **49**, 1749–1755.
4 A. van Belkum, C. D. Burnham and J. W. A. Rossen, *et al.*, *Nat. Rev. Microbiol.*, 2020, **18**, 299–311.
5 A. van Belkum and W. M. Dunne, *J. Clin. Microbiol.*, 2013, **51**, 2018.
6 O. Opota, A. Croxatto, G. Prod'hom and G. Greub, *Clin. Microbiol. Infect.*, 2015, **21**, 313–322.
7 S. Wang, F. Inci, T. L. Chaunzwa, A. Ramanujam, A. Vasudevan, S. Subramanian, A. Chi Fai Ip, B. Sridharan, U. A. Gurkan and U. Demirci, *Int. J. Nanomed.*, 2012, **7**, 2591–2600.
8 G. Longo, L. Alonso-Sarduy, L. M. Rio, A. Bizzini, A. Trampuz, J. Notz, G. Dietler and S. Kasas, *Nat. Nanotechnol.*, 2013, **8**, 522–526.
9 H. Etayash, M. F. Khan, K. Kaur and T. Thundat, *Nat. Commun.*, 2016, **7**, 12947.
10 M. W. Kadlec, D. You, J. C. Liao and P. K. Wong, *J. Lab. Autom.*, 2013, **19**, 258–266.
11 W.-B. Lee, C.-C. Chien, H.-L. You, F.-C. Kuo, M. S. Lee and G.-B. Lee, *Lab Chip*, 2019, **19**, 2699–2708.
12 S. Kim, F. Masum, J.-K. Kim, H. J. Chung and J. S. Jeon, *Lab Chip*, 2019, **19**, 959–973.
13 L. Baraban, F. Bertholle, M. L. M. Salverda, N. Bremond, P. Panizza, J. Baudry, J. A. G. M. de Visser and J. Bibette, *Lab Chip*, 2011, **11**, 4057–4062.
14 L. Cui, D. Zhang, K. Yang, X. Zhang and Y.-G. Zhu, *Anal. Chem.*, 2019, **91**, 15345–15354.
15 K. Wang, S. Li, M. Petersen, S. Wang and X. Lu, *Nanomaterials*, 2018, **8**, 762.
16 C. Y. Liu, Y. Y. Han, P. H. Shih, W. N. Lian, H. H. Wang, C. H. Lin, P. R. Hsueh, J. K. Wang and Y. L. Wang, *Sci. Rep.*, 2016, **6**, 23375.
17 K.-W. Chang, H.-W. Cheng, J. Shiue, J.-K. Wang, Y.-L. Wang and N.-T. Huang, *Anal. Chem.*, 2019, **91**, 10988–10995.
18 P. Kinnunen, B. H. McNaughton, T. Albertson, I. Sinn, S. Mofakham, R. Elbez, D. W. Newton, A. Hunt and R. Kopelman, *Small*, 2012, **8**, 2477–2482.
19 R. Kargupta, S. Puttaswamy, A. J. Lee, T. E. Butler, Z. Li, S. Chakraborty and S. Sengupta, *Biol. Res.*, 2017, **50**, 21.
20 Y. Yang, K. Gupta and K. L. Ekinci, *Proc. Natl. Acad. Sci. U. S. A.*, 2020, **117**, 10639.
21 U. von Ah, D. Wirz and A. U. Daniels, *BMC Microbiol.*, 2009, **9**, 106.
22 Y. Matsumoto, S. Sakakihara, A. Grushnikov, K. Kikuchi, H. Noji, A. Yamaguchi, R. Iino, Y. Yagi and K. Nishino, *PLoS One*, 2016, **11**, e0148797.
23 J. Choi, Y.-G. Jung, J. Kim, S. Kim, Y. Jung, H. Na and S. Kwon, *Lab Chip*, 2013, **13**, 280–287.
24 H. W. Hou, R. P. Bhattacharyya, D. T. Hung and J. Han, *Lab Chip*, 2015, **15**, 2297–2307.
25 S. Wang, F. Inci, T. L. Chaunzwa, A. Ramanujam, A. Vasudevan, S. Subramanian, A. Chi Fai Ip, B. Sridharan, U. Gurkan and U. Demirci, *Portable microfluidic chip for detection of Escherichia coli in produce and blood*, 2012.
26 Y. Marcy, T. Ishoey, R. S. Lasken, T. B. Stockwell, B. P. Walenz, A. L. Halpern, K. Y. Beeson, S. M. D. Goldberg and S. R. Quake, *PLoS Genet.*, 2007, **3**, e155.
27 J. Q. Boedicker, L. Li, T. R. Kline and R. F. Ismagilov, *Lab Chip*, 2008, **8**, 1265–1272.
28 R. H. Hansen, A. C. Timm, C. M. Timm, A. N. Bible, J. L. Morrell-Falvey, D. A. Pelletier, M. L. Simpson, M. J. Doktycz and S. T. Retterer, *PLoS One*, 2016, **11**, e0155080.
29 N.-T. Huang, Y.-J. Hwong and R. L. Lai, *Microfluid. Nanofluid.*, 2018, **22**, 16.
30 W. R. Premasiri, J. C. Lee, A. Sauer-Budge, R. Théberge, C. E. Costello and L. D. Ziegler, *Anal. Bioanal. Chem.*, 2016, **408**, 4631–4647.
31 C.-Y. Liu, Y.-Y. Han, P.-H. Shih, W.-N. Lian, H.-H. Wang, C.-H. Lin, P.-R. Hsueh, J.-K. Wang and Y.-L. Wang, *Sci. Rep.*, 2016, **6**, 23375.
32 M. Morháč and V. Matoušek, *Appl. Spectrosc.*, 2008, **62**, 91–106.
33 S. C. Kim, S. Cestellos-Blanco, K. Inoue and R. N. Zare, *Antibiotics*, 2015, **4**, 455–466.